Interface electronic structures of $BaTiO_3@X$ nanoparticles ($X=\gamma$-Fe_2O_3, Fe_3O_4, α-Fe_2O_3, and Fe) investigated by XAS and XMCD

D. H. Kim,[1] H. J. Lee,[1] G. Kim,[1] Y. S. Koo,[2] J. H. Jung,[2] H. J. Shin,[3] J.-Y. Kim,[3] and J.-S. Kang[1,*]
[1]*Department of Physics, The Catholic University of Korea, Bucheon 420-743, Korea*
[2]*Department of Physics, Inha University, Incheon 402-751, Korea*
[3]*Pohang Accelerator Laboratory (PAL), POSTECH, Pohang 790-784, Korea*
(Received 13 October 2008; revised manuscript received 26 November 2008; published 6 January 2009)

The electronic structures of $BaTiO_3@X$ (core@shell) nanoparticles ($X=\gamma$-Fe_2O_3, Fe_3O_4, and Fe) have been investigated by employing soft x-ray-absorption spectroscopy and x-ray magnetic circular dichroism (XMCD). It is found that the valence states of Ti ions near interfaces are formally tetravalent (Ti^{4+}:$3d^0$) and that the valence states of Fe ions in shells are essentially the same as those of the corresponding *bulk* materials, with some disorder in the site occupations for $X=\gamma$-Fe_2O_3 and Fe_3O_4. The negligible Ti $2p$ XMCD signals were observed, indicating that the induced spin polarization of the interface Ti $3d$ electrons is negligible in $BaTiO_3@X$ nanoparticles.

DOI: 10.1103/PhysRevB.79.033402 PACS number(s): 73.22.−f, 78.70.Dm, 87.64.ku

Nanocomposite materials are considered to be possible candidates for multifunctional materials, having both magnetic and ferroelectric properties.[1,2] It has been found that the appropriate shaping and sintering of the ferroelectric-based artificial nanoscale heterostructures enable a tuning of physical properties,[3] for which interfaces are considered to play a key role. First-principles calculations for $BaTiO_3$/Fe multilayers[4] predicted the change in the interface magnetization under the ferroelectric displacement of $BaTiO_3$ and obtained the induced magnetic moments on the interface Ti ions. However, the predicted induced magnetic moments on the interface Ti ions have not been experimentally confirmed yet. Recently the interesting magnetodielectric coupling has been observed in core@shell-type $BaTiO_3@\gamma$-Fe_2O_3 nanoparticles,[5] depending on the shell thickness, the lattice mismatch near interfaces, and temperature.

In order to understand the origin of the magnetoelectric coupling in $BaTiO_3/X$ multilayers or $BaTiO_3@X$ (core@shell)-type nanoparticles, it is important to investigate their electronic structures, such as the valence and spin states of transition-metal (T) ions in X and the induced spin polarization of Ti ions near the interfaces. Soft x-ray-absorption spectroscopy (XAS) (Refs. 6 and 7) and soft x-ray magnetic circular dichroism (XMCD) (Refs. 8 and 9) are powerful experimental tools for studying the valence states and the element-specific magnetic moments of T ions in solids, respectively. In this work, we have investigated the electronic structures of core@shell ferrite nanoparticles of $BaTiO_3@X$ ($X=\gamma$-Fe_2O_3, Fe_3O_4, and Fe) by employing XAS and XMCD with synchrotron radiation. In particular, we have tried to measure the induced spin polarization of the interface Ti ions by performing XMCD measurements.

Core@shell-type $BaTiO_3@X$ nanoparticles ($X=\gamma$-Fe_2O_3, Fe_3O_4, and Fe) were synthesized by a sonochemical method. The details of the synthesis and the characterization of $BaTiO_3@X$ nanoparticles are described in Refs. 5 and 10. The average size of cores and the average thickness of shells were ~70 and ~20 nm, respectively.[5,10] XAS data were obtained at both 8A1 and 2A undulator beamlines at the Pohang Accelerator Laboratory (PAL) both at room temperature and at $T\sim 80$ K with the total resolution less than 100 meV at $h\nu\sim 500$ eV. XMCD experiments[11] were performed at the 2A beamline at the PAL by using the circularly polarized light with a degree of circular polarization >90%. XMCD spectra were obtained at $T\sim 80$ K under the applied magnetic field of ~0.7 T. The total resolution for XMCD was ~120 meV at $h\nu\sim 700$ eV. Base pressure was better than $\sim 5\times 10^{-10}$ Torr. XAS and XMCD spectra were collected in the total electron yield mode, which has a probing depth of $\leq\sim 10$ nm.

Figure 1 shows the measured Fe $2p$ XAS spectra (dots) of $BaTiO_3@X$ ($X=\alpha$-Fe_2O_3, γ-Fe_2O_3, Fe_3O_4, and Fe), which are divided into L_3 ($2p_{3/2}$) and L_2 ($2p_{1/2}$) regions. These are compared to the Fe $2p$ XAS spectra (solid lines) of parent *bulk* materials: α-Fe_2O_3,[12] γ-Fe_2O_3,[12,13] Fe_3O_4,[14] and Fe metal (our own data).[15] This comparison shows that the present Fe $2p$ XAS spectra of $BaTiO_3@X$ for $X=\alpha$-Fe_2O_3 and Fe_3O_4 are very similar to those of bulk α-Fe_2O_3 and Fe_3O_4, respectively, while that for $X=\gamma$-Fe_2O_3 shows a small difference in the intensity of the low-energy peak (A) in the L_3 absorption edge compared to that of bulk γ-Fe_2O_3. Fe ions in both α-Fe_2O_3 and γ-Fe_2O_3 are formally trivalent (Fe^{3+}), and the differences in the line shapes between the two are due to the different site occupations;[11,16] Fe ions in α-Fe_2O_3 occupy the octahedral (O_h) sites only, while Fe ions in γ-Fe_2O_3 occupy both the O_h and tetrahedral (T_d) sites. The sharper and larger intensity of the low-energy peak (A) in L_3 for α-Fe_2O_3 is due to the O_h-site occupation of Fe ions. Hence the larger intensity of the peak A in our $X=\gamma$-Fe_2O_3, as compared to *bulk* γ-Fe_2O_3, indicates that Fe ions in $BaTiO_3@\gamma$-Fe_2O_3 nanoparticles occupy O_h sites more than in bulk γ-Fe_2O_3.

The Fe $2p$ XAS line shape of Fe_3O_4 is a little different from those of α-Fe_2O_3 and γ-Fe_2O_3 due to the existence of divalent Fe^{2+} ions in Fe_3O_4. In particular, the extra-shoulder-like features in the low-energy sides (marked with arrows) arise from the existence of the Fe^{2+} states.[14] As compared to bulk Fe_3O_4, the Fe $2p$ XAS for $BaTiO_3@Fe_3O_4$ exhibits a slightly weaker intensity for the peak A but with the same intensities for the low-energy shoulders (arrows). Considering the discussion above, such differences indicate that the O_h-site occupation of Fe^{3+} ions in our $BaTiO_3@Fe_3O_4$ is

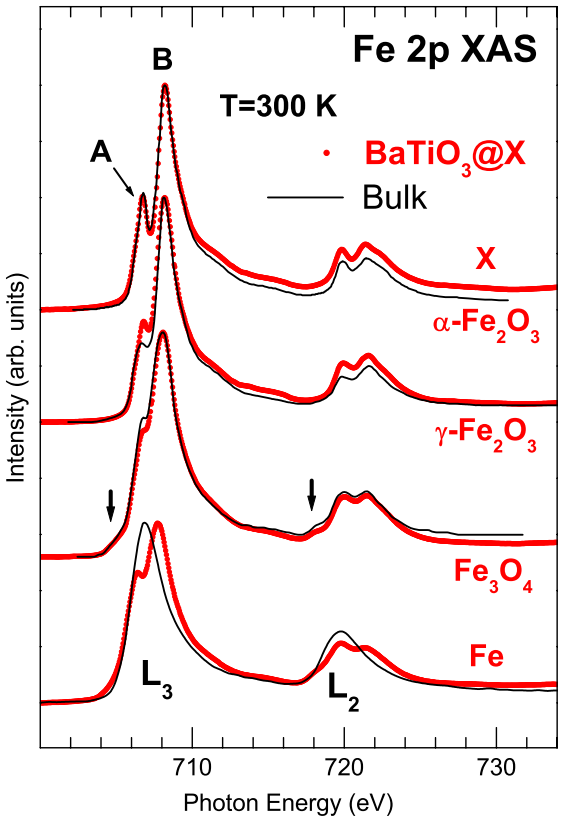

FIG. 1. (Color online) Comparison of the Fe $2p$ XAS spectra (dots) of $BaTiO_3@X$ with the corresponding bulk materials (solid lines).

less than in bulk Fe_3O_4 but that the relative amount of Fe^{2+} ions with respect to Fe^{3+} ions is the same in $BaTiO_3@Fe_3O_4$ and bulk Fe_3O_4. This conclusion is supported by the Fe $2p$ XMCD study (see Fig. 2). Finally, the Fe $2p$ XAS spectrum for $X=$Fe exhibits the extramultiplet features, as compared to pure Fe metal, which is because the metallic Fe shell is slightly oxidized.[17] To sum up, the Fe $2p$ XAS spectra of $BaTiO_3@X$ nanoparticles reveal that the Fe-based shells maintain their original valence states of the corresponding bulk materials. This finding is consistent with that of Fig. 2 below.

Figure 2(a) shows the measured Fe $2p$ XAS spectra of $BaTiO_3@\gamma$-Fe_2O_3, obtained with different photon helicities: ρ_+ (red) and ρ_- (blue). Also shown are the Fe $2p$ XMCD spectrum (middle panel), which corresponds to $\Delta\rho=\rho_+-\rho_-$ (red lines) with its integrated value (black dotted lines). At the bottom panel the sum (red lines) of $\rho_++\rho_-$, corresponding to the Fe $2p$ XAS, and its integrated value (black dotted lines) are shown. The resulting Fe $2p$ XMCD spectrum of $BaTiO_3@\gamma$-Fe_2O_3 is similar to that of bulk γ-Fe_2O_3 [see Fig. 2(b)],[11] indicating that the valence and spin states of Fe ions in $BaTiO_3@\gamma$-Fe_2O_3 nanoparticles are similar to those of bulk γ-Fe_2O_3.

Figure 2(b) compares the Fe $2p$ XMCD spectra ($\Delta\rho=\rho_+-\rho_-$) of $BaTiO_3@X$ ($X=\gamma$-Fe_2O_3, Fe_3O_4, and Fe), which were determined as in Fig. 2(a). In order to find the effects of nanosize particles, we also compare these spectra with the corresponding Fe $2p$ XMCD spectra of bulk γ-Fe_2O_3,[12] bulk Fe_3O_4,[18] and bulk Fe (our own data).[15] The complicated features in the L_3 absorption edges of $X=\gamma$-Fe_2O_3 and Fe_3O_4 are due to the antiparallel spin orientations between O_h and T_d sites in γ-Fe_2O_3 and Fe_3O_4,[11,18] which are labeled as O and T in Fig. 2(b), respectively. Here any FeO phase in $X=Fe_3O_4$ does not contribute to the Fe $2p$ XMCD because FeO is antiferromagnetic.

The Fe $2p$ XMCD spectra of $BaTiO_3@X$ nanoparticles provide experimental evidence that the shells are ferrimagnetic for $X=\gamma$-Fe_2O_3 and Fe_3O_4. The Fe $2p$ XMCD spectrum of $X=\gamma$-Fe_2O_3 is very similar to that of bulk γ-Fe_2O_3, except for the slightly larger XMCD signal for O_h sites. This feature in Fe $2p$ XMCD is consistent with that for Fe $2p$ XAS in Fig. 1, that is, $BaTiO_3@\gamma$-Fe_2O_3 nanoparticles occupy the more O_h sites than in bulk γ-Fe_2O_3. On the other hand, the Fe $2p$ XMCD for $X=Fe_3O_4$ exhibits weaker negative octahedral peaks (O) than in bulk Fe_3O_4, suggesting that the O_h-site occupation of Fe^{3+} ions in $BaTiO_3@Fe_3O_4$ is smaller than in bulk Fe_3O_4. Since the XMCD amplitude is site-specific, the weaker octahedral peaks (O) in $BaTiO_3@Fe_3O_4$ than in bulk Fe_3O_4 indicate the reduced magnetic moment[18] in $BaTiO_3@Fe_3O_4$ than in bulk Fe_3O_4. Note, however, that the intensity ratios between two octahedral peaks (O) in $BaTiO_3@X$ for both $X=Fe_3O_4$ and γ-Fe_2O_3 are different from those in their bulk oxides, implying that the size effect in the ferrimagnetic shells is not simple. It is expected that the interface mixing causes disorder in the spin arrangement among different sites in $BaTiO_3@X$ nanoparticles.

The XMCD spectrum of $BaTiO_3@$Fe is also qualitatively similar to that of bulk Fe metal, indicating that the magnetic moments of Fe ions in the shell are coupled ferromagnetically. However, the detailed XMCD spectrum of $BaTiO_3@$Fe is somewhat different from that of pure Fe metal, which is due to the partial oxidation of Fe in the shell.[17] To sum up, the XMCD spectra for $BaTiO_3@X$ nanoparticles in Fig. 2 provide evidence that the shells are ferrimagnetic for $X=\gamma$-Fe_2O_3 and Fe_3O_4, and ferromagnetic for $X=$Fe. Further, the Fe $2p$ XMCD spectra for $BaTiO_3@X$ show the existence of the disorder in the site occupancy for $X=\gamma$-Fe_2O_3 and Fe_3O_4, as compared to their bulk materials, even though the valence states of the Fe ions in the ferrimagnetic shells are the same as those of the corresponding bulk materials.

Figure 3(a) compares the measured Ti $2p$ XAS spectra of $BaTiO_3@X$ ($X=$Fe, γ-Fe_2O_3, and Fe_3O_4) with that of bulk TiO_2 powder[19] and the calculated XAS for a Ti^{4+} ion in the O_h symmetry with the crystal-field splitting 10 Dq of 1.8 eV (Ref. 20). A very good agreement is found between the measured Ti $2p$ XAS spectra of $BaTiO_3@X$ and the calculated Ti $2p$ XAS for a Ti^{4+} ion in the O_h symmetry. Further, the Ti $2p$ XAS spectra of $BaTiO_3@X$ are nearly identical to one another for all X. Therefore Fig. 3(a) justifies the tetravalent Ti^{4+} ($3d^0$) states in $BaTiO_3@X$. Considering the probing depth of XAS ($\leq\sim10$ nm) and the average shell thickness of $BaTiO_3@X$ nanoparticles ($\sim$20 nm), these Ti $2p$ XAS signals come mostly from interfaces. Therefore this comparison provides evidence that Ti ions near the interfaces of $BaTiO_3@X$ are formally tetravalent (Ti^{4+}:$3d^0$). As will be discussed below, we think that these valence states of Ti ions are important in determining the physical properties of $BaTiO_3@X$ nanoparticles.

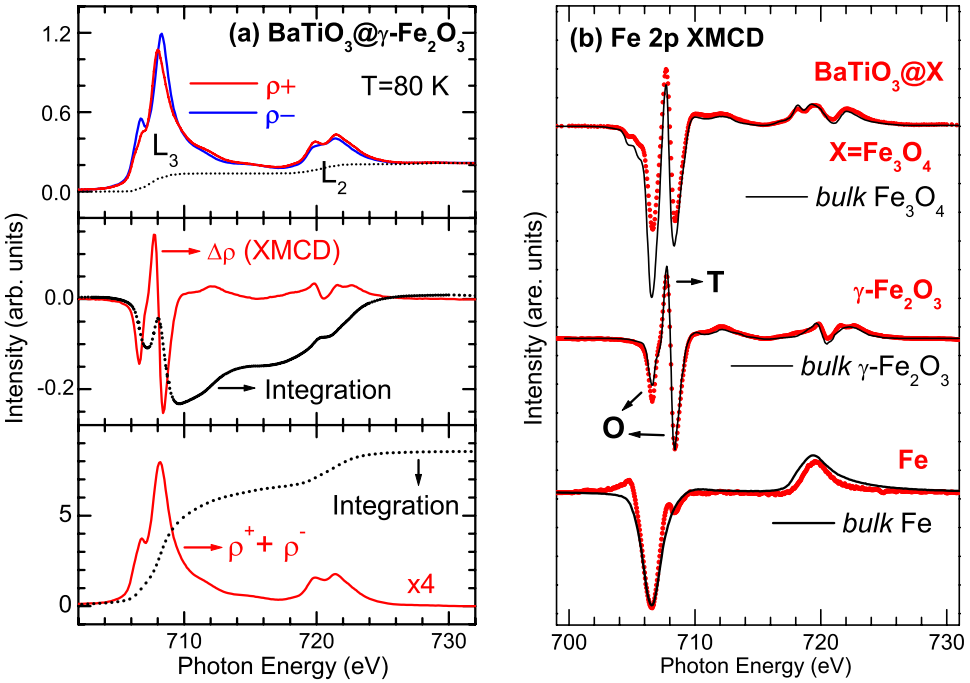

FIG. 2. (Color online) (a) The Fe $2p$ XMCD data for $BaTiO_3$@ γ-Fe_2O_3. See the text for details. (b) Comparison of the Fe $2p$ XMCD ($\Delta\rho=\rho_+-\rho_-$) spectra (dots) of $BaTiO_3$@X to those of their bulk materials (solid lines).

As predicted in Ref. 4, the interface Ti ions of $BaTiO_3$@X might exhibit the induced spin polarization if the shells are ferromagnetic (X=Fe) or ferrimagnetic (X = γ-Fe_2O_3 and Fe_3O_4). In order to check how large the induced spin polarization of the interface Ti ions is, we have performed Ti $2p$ XMCD measurements for $BaTiO_3$@X. Note that in Fig. 3(a), the scale factor[21] of the Ti $2p$ XAS spectrum increases from 1 for X=Fe to ~25–28 for X = Fe_3O_4 and γ-Fe_2O_3. This trend indicates that the average thickness of the shell increases from X=Fe to X=Fe_3O_4 $\approx X=\gamma$-Fe_2O_3 since the Ti-related signals come from interfaces.[22,23] The largest Ti $2p$ XAS intensity for $BaTiO_3$@Fe arise from the thinnest shell thickness for X =Fe among $BaTiO_3$@X.

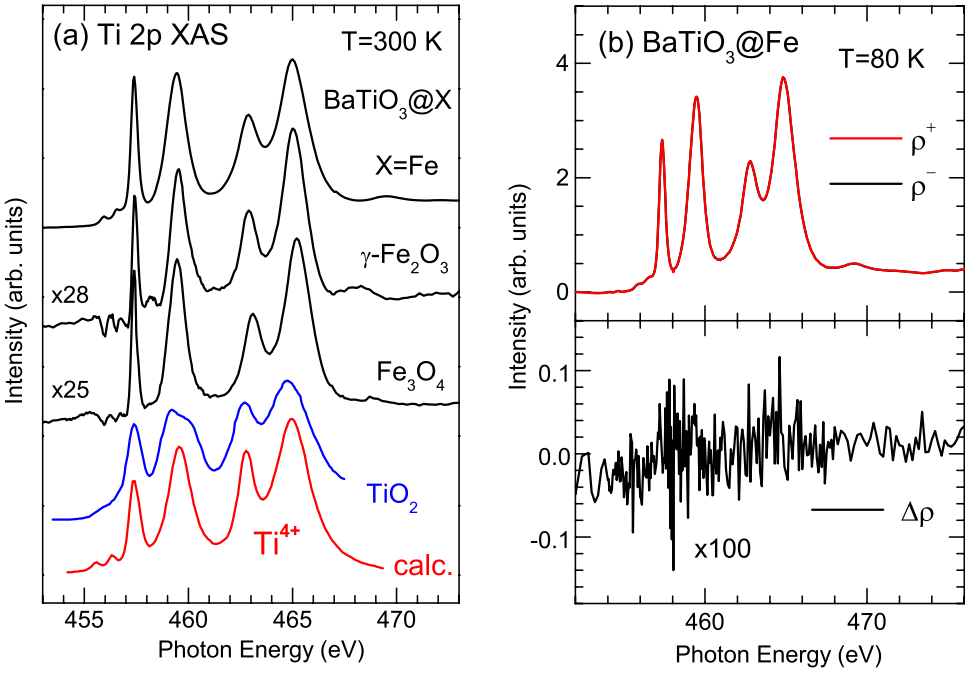

FIG. 3. (Color online) (a) Comparison of the Ti $2p$ XAS spectra of $BaTiO_3$@X, bulk TiO_2 (Ref. 19), and the calculated Ti $2p$ XAS for a Ti^{4+} ion in the O_h symmetry (Ref. 20). (b) (Upper) Ti $2p$ ρ_+ (red) and ρ_- (black) for $BaTiO_3$@Fe. (Lower) The corresponding Ti $2p$ XMCD, $\Delta\rho=\rho_+-\rho_-$.

The upper and lower panels of Fig. 3(b) show the Ti $2p$ ρ_+ (red) and ρ_- (black), and the Ti $2p$ XMCD ($\Delta\rho=\rho_+-\rho_-$) for $BaTiO_3$@Fe, respectively. Figure 3(b) exhibits the almost zero Ti $2p$ XMCD signals for $BaTiO_3$@Fe, indicating that the induced spin polarization of Ti $3d$ electrons near the interface is negligibly small. Such a weak dichroism is consistent with the tetravalent (Ti^{4+}) states of the interface Ti ions because Ti^{4+} ions have no occupied $3d$ electrons in the ground states ($3d^0$), and so there are no d electrons available for the induced spin polarization. Our finding suggests that the core-shell coupling at $BaTiO_3$@X nanoparticles is not strong enough to modify their interface electronic structures substantially, so the subtle changes are not detectable by XAS or XMCD at finite temperature even though the zero-temperature calculations for $Fe/BaTiO_3$ multilayers predicted the induced magnetic moments on the interface Ti atoms.[4] That is, our study shows that the induced spin polarization of the interface Ti $3d$ electrons in $BaTiO_3$@X nanoparticles is too weak at finite temperature to invoke the interface-driven multiphysical properties in $BaTiO_3$@X. The negligible XMCD feature in Fig. 3(b), however, does not rule out the possibility of the interface Ti ions having induced magnetic moments of sp character. In this aspect, the XMCD measurement of the Ti $1s$ (K) edge would be useful to check the above possibility.

In conclusion, the electronic structures of $BaTiO_3$@X ferromagnetic nanoparticles ($X=\gamma$-Fe_2O_3, Fe_3O_4, and Fe) have been investigated by employing XAS and XMCD with synchrotron radiation. T $2p$ XAS spectra (T=Fe, Ti) show that the valence states of Fe ions in the shells are very similar to those of bulk γ-Fe_2O_3, Fe_3O_4, and Fe, within the experimental uncertainties, and that Ti ions near the interfaces are formally tetravalent (Ti^{4+}:$3d^0$). Fe $2p$ XMCD measurements reveal that Fe ions in the shells are ferrimagnetic for $X=\gamma$-Fe_2O_3 and Fe_3O_4, and ferromagnetic for X=Fe. The disorder in the site occupancy has been found in $BaTiO_3$@X nanoparticles for $X=\gamma$-Fe_2O_3 and Fe_3O_4, as compared to their bulk materials. Contrary to the theoretical prediction, the dichroic effect in the interface Ti $2p$ XMCD spectra is almost negligible, indicating that the induced spin polarization of the interface Ti $3d$ electrons is negligibly weak in $BaTiO_3$@X nanoparticles. This finding is consistent with the tetravalent Ti^{4+} ions that have the $3d^0$ ground-state configuration.

This work was supported by KRF (Grant No. KRF-2006-311-C00277), by the Korean Government (MOEHRD) through KRF (Grant No. KRF-2005-070-C00053), and in part by the Department Specialization Fund of the CUK (2008). PAL is supported by the MOST and POSCO in Korea.

*Corresponding author. kangjs@catholic.ac.kr

[1] D. Grosso, C. Boissiere, B. Smarsly, T. Brezensinski, N. Pinna, P. Albouy, H. Amenitsch, and C. Sanchez, Nature Mater. **3**, 787 (2004).
[2] H. Zheng, J. Wang, S. E. Lofland, Z. Ma, L. Mohaddes-Ardabili, T. Zhao, L. Salamanda-Riba, S. R. Shinde, S. B. Shinde, S. B. Ogale, F. Bai, D. Viehland, Y. Jia, D. G. Schlom, M. Wuttig, A. Roytburd, and R. Ramesh, Science **303**, 661 (2004).
[3] S. Mornet, C. Elissalde, O. Bidault, F. Weill, E. Sellier, O. Nguyen, and M. Maglione, Chem. Mater. **19**, 987 (2007).
[4] C. G. Duan, S. S. Jaswal, and E. Y. Tsymbal, Phys. Rev. Lett. **97**, 047201 (2006).
[5] Y. S. Koo, T. Bonaedy, K. D. Sung, J. H. Jung, J. B. Yoon, Y. H. Jo, M. H. Jung, H. J. Lee, T. Y. Koo, and Y. H. Jeong, Appl. Phys. Lett. **91**, 212903 (2007).
[6] F. M. F. de Groot, J. C. Fuggle, B. T. Thole, and G. A. Sawatzky, Phys. Rev. B **42**, 5459 (1990).
[7] G. van der Laan and I. W. Kirkman, J. Phys.: Condens. Matter **4**, 4189 (1992).
[8] B. T. Thole, P. Carra, F. Sette, and G. van der Laan, Phys. Rev. Lett. **68**, 1943 (1992).
[9] C. T. Chen, Y. U. Idzerda, H.-J. Lin, N. V. Smith, G. Meigs, E. Chaban, G. H. Ho, E. Pellegrin, and F. Sette, Phys. Rev. Lett. **75**, 152 (1995).
[10] Y. S. Koo, D. H. Kim, and J. H. Jung, J. Korean Phys. Soc. **48**, 677 (2006).
[11] J.-S. Kang, G. Kim, H. J. Lee, D. H. Kim, H. S. Kim, J. H. Shim, S. Lee, H. G. Lee, J. Y. Kim, B. H. Kim, and B. I. Min, Phys. Rev. B **77**, 035121 (2008).
[12] J.-Y. Kim, T. Y. Koo, and J.-H. Park, Phys. Rev. Lett. **96**, 047205 (2006).
[13] T. J. Regan, H. Ohldag, C. Stamm, F. Nolting, J. Lüning, J. Stöhr, and R. L. White, Phys. Rev. B **64**, 214422 (2001).
[14] K. Kuepper, I. Balasz, H. Hesse, A. Winiarski, K. C. Prince, M. Matteucci, D. Wett, R. Szargan, E. Burzo, and M. Neumann, Phys. Status Solidi A **201**, 3252 (2004).
[15] The Fe $2p$ XAS and XMCD spectra of our bulk Fe metal are essentially the same as those in Ref. 9.
[16] J. P. Crocombette, M. Pollak, F. Jollet, N. Thromat, and M. Gautier-Soyer, Phys. Rev. B **52**, 3143 (1995).
[17] We did not sputter clean $BaTiO_3$@Fe. Sputter cleaning would remove the oxidized surface.
[18] M. Pilard, O. Ersen, S. Cherifi, B. Carvello, L. Roiban, B. Muller, F. Scheurer, L. Ranno, and C. Boeglin, Phys. Rev. B **76**, 214436 (2007).
[19] L. Soriano, M. Abbate, J. Vogel, J. C. Fuggle, A. Ferández, A. R. González-Dlipe, M. Sacchi, and J. M. Sanz, Surf. Sci. **290**, 427 (1993).
[20] F. M. F. de Groot, J. C. Fuggle, B. T. Thole, and G. A. Sawatzky, Phys. Rev. B **41**, 928 (1990).
[21] Each Ti $2p$ XAS was normalized with respect to the intensity of the corresponding Fe $2p$ XAS. Then these scale factors were determined by making the Ti $2p$ peak heights roughly the same.
[22] J.-S. Kang, D. W. Hwang, J. H. Hong, J. I. Jeong, H. K. Park, J. H. Moon, Y. P. Lee, P. Benning, C. G. Olson, S. J. Youn, and B. I. Min, Phys. Rev. B **51**, 1039 (1995), and see Ref. 32 therein.
[23] H.-J. Kim, J.-H. Park, and E. Vescovo, Phys. Rev. B **61**, 15284 (2000), and see Ref. 15 therein.